

Aus der Klinik für Psychiatrie und Psychotherapie
der Medizinischen Fakultät Charité – Universitätsmedizin Berlin

DISSERTATION

Effects of stimulus degradation on neural object processing in the two
visual pathways

zur Erlangung des akademischen Grades
Doctor medicinae (Dr. med.)

vorgelegt der Medizinischen Fakultät
Charité – Universitätsmedizin Berlin

von

Natasha Darcy
aus München

Datum der Promotion: 06.03.2020

INDEX

Abstract	3
Zusammenfassung	4
1. Introduction	5
2. Methods	7
2.1 <i>Participants & Setup</i>	7
2.2 <i>Stimuli</i>	8
2.3 <i>Procedure</i>	10
2.4 <i>Analysis</i>	12
2.4.1 <i>Behavioural analysis</i>	12
2.4.2 <i>FMRI analysis</i>	12
2.4.3 <i>Statistical analysis</i>	13
3. Results	14
3.1 <i>Behavioural results</i>	14
3.1.1 <i>Subjective</i>	14
3.1.2 <i>Objective</i>	15
3.2 <i>FMRI results</i>	16
3.2.1 <i>Main multivariate pattern analysis</i>	16
3.2.2 <i>Hemispheric analysis</i>	18
3.2.3 <i>Univariate analysis</i>	18
3.2.5 <i>Awareness analysis</i>	19
4. Discussion	21
4.1 <i>Summary of results</i>	21
4.2 <i>Relation to previous findings</i>	21
4.3 <i>Secondary observations and limitations</i>	22
4.4 <i>Connectivity and temporal dynamics</i>	23
4.5 <i>Updated theories and future considerations</i>	25
References	26
Eidesstattliche Versicherung	29
Auszug aus der Journal Summary List	30
Publikation	31
Lebenslauf	40
Publikationsliste	41
Danksagung	42

Abstract

(englisch)

Roughly three decades ago, Goodale and Milner proposed the highly influential Two streams hypothesis, which separates visual processing into ventral "vision for perception" and dorsal "vision for action" pathways. According to the theory, the latter distinguishes itself by its capability to process visual content without awareness. Information on object category is found in both pathways and enables targeted functional imaging of neural object processing with appropriate stimulus images. A substantial branch of research has examined how object processing in each stream differs when stimuli are suppressed from awareness, most often in dichotomous visible-versus-invisible designs using a specific method of interocular suppression, Continuous flash suppression (CFS). A few studies have reported intact processing of suppressed information in the dorsal pathway. Yet overall, the evidence regarding differences between the pathways under CFS has been inconclusive. In a renewed approach we aimed to exclude method-specific effects and adopted an alternative means of stimulus degradation. Applying visual noise to modulate stimulus information of tools and faces parametrically, we conducted a functional magnetic resonance imaging (fMRI) experiment, testing for differential processing of degraded stimuli in the two visual pathways. Our multivariate results and Bayesian statistical analysis supported a linear association of stimulus signal and functional activity in both visual pathways, albeit with lower absolute measures of stimulus encoding in dorsal regions. In line with the current notions of interaction and integration in the realm of high-level visual processing, the noise paradigm used in this study provided no evidence for differences in degraded object processing between the two visual pathways.

Zusammenfassung

(deutsch)

Vor etwa drei Jahrzehnten stellten Goodale und Milner die einflussreiche Theorie der zwei visuellen Pfade auf, die eine Aufteilung der visuellen Verarbeitung in einen ventralen ("Sehen zur Wahrnehmung") und einen dorsalen Pfad ("Sehen zur Handlung") beschreibt. Laut ihrer Theorie zeichnet sich letzterer dadurch aus, dass die Verarbeitung visueller Inhalte auch unbewusst ablaufen kann. Informationen über Objektkategorien finden sich in beiden Pfaden, sodass eine gezielte funktionelle Bildgebung mit geeigneten Stimuli ermöglicht wird. Ein beachtlicher Forschungsbereich untersucht Unterschiede in der Objektverarbeitung zwischen den beiden Pfaden, wenn die bewusste Wahrnehmung der Stimuli unterdrückt wird. Die hierbei am häufigsten genutzte Methode ist interokuläre Suppression, insbesondere Continuous Flash Suppression (CFS), wobei Stimuli meist dichotom als sichtbar oder unsichtbar gelten. Bisherige CFS-Studien lieferten bezüglich potentieller Differenzen zwischen den Pfaden, vornehmlich der intakten Verarbeitung unterdrückter Information ausschließlich im dorsalen Pfad, uneinheitliche Ergebnisse. Um die beobachteten Unterschiede unabhängig von der bisherigen Methode zu prüfen, verwendeten wir in dieser Studie eine alternative Suppressionsmethode. Mittels Bildrauschen modulierten wir Bildinformation von Werkzeug- und Gesichtstimuli in parametrischen Abstufungen und führten eine neue fMRT-Studie durch, um Unterschiede in der Verarbeitung von degradierten Stimuli zwischen den beiden Pfaden zu eruieren. Unsere multivariaten Ergebnisse und die bayesianische statistische Analyse zeigten in beiden visuellen Pfaden eine lineare Abhängigkeit der funktionellen Aktivität vom Stimulussignal, wobei dorsale Regionen geringere absolute Werte der Stimulusverarbeitung aufwiesen. Im Einklang mit der gegenwärtigen Tendenz zur Interaktion und Integration im Bereich der höheren visuellen Verarbeitung, konnte dieses Paradigma bezüglich der Verarbeitung von Objektkategorien keinen Nachweis für Unterschiede zwischen den beiden visuellen Pfaden erbringen.

1. Introduction

Vision, widely considered the dominant human sense in Western society (Classen, 1997, San Roque et al., 2015), occupies a central role both in our perception of the world and in neuroscientific research. In our fellow primate, the macaque, the proportion of overall cerebral cortex dedicated to visual processing was estimated at 52% (Felleman and Van Essen, 1991). It is likely that our own cortex devotes a similarly impressive fraction of processing power to this complex sensory modality. Therefore, investigating the structure and function of these manifold cortical areas is a major goal in cognitive neuroscience. Current expansive fields include research on extrastriate retinotopic processing, on visual attention, visual memory and intricate abilities such as object processing.

In this latter field, the influential ‘Two visual streams hypothesis’ (TVSH) was proposed by Goodale and Milner (1992) roughly three decades ago. Based on prior work by Ungerleider and Mishkin (1982), they postulated that the higher-order visual system is split into two functional pathways with different purposes. The occipito-temporal or ventral stream was termed ‘vision for perception’, determining the ‘what’ of our conscious vision (figure 1A). The occipito-parietal or dorsal ‘vision for action’ stream tells us ‘where’ or ‘how’. The latter enables spatial visual attention in the viewer's reference frame, and thus movements like grasping or eye saccades. Crucially, they deemed that processing in this pathway could remain unconscious. This phenomenon was exemplified by patient DF, who had bilateral lesions in regions within the ventral stream (figure 1B) and could grasp objects accurately without consciously perceiving them (Goodale et al., 1991).

Both streams can be targeted experimentally by presenting certain object categories. The fusiform face area is a classic example of a category-selective area in the ventral stream (Kanwisher et al., 1997). Visual presentation of faces, regardless of orientation, characteristics or current task, reliably induces activity in this region (Kanwisher, 2010). Dorsal areas

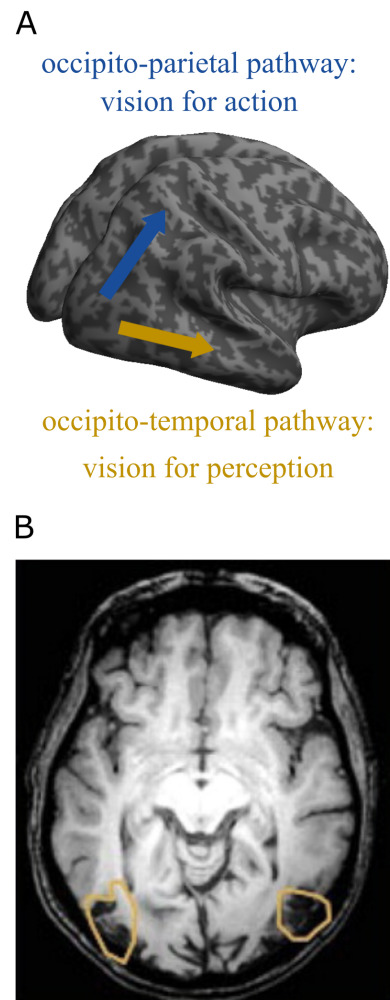


Figure 1. A) Visualisation of the ‘Two visual streams hypothesis’ proposed by Goodale and Milner (1992). B) Lesions in Patient DF’s ventral pathway (James et al., 2003).

have also demonstrated processing of object categories. Since these areas have been characterised as action-related, manipulable objects such as tools are favoured in this instance (Culham et al., 2003). As in the ventral pathway, dorsal object processing does not rely on specific orientations or shapes, but rather on category itself, though activity patterns varied with different tasks such as viewing, grasping and reaching (Macdonald and Culham, 2015, Freud et al., 2016).

To examine one of the most interesting discrepancies between the streams, namely the dissociation of dorsal processing from awareness, a multitude of studies have used various methods to degrade or “hide” visual input from consciousness and measure residual processing. In the ventral pathway, the relationship between conscious perception and functional activity is approximately linear and highly consistent. A decrease in visibility such that conscious perception is diminished results in weaker cortical representation of category information (Grill-Spector et al., 2000, Tjan et al., 2006).

In the dorsal stream however, a number of authors have shown preserved functional activity when participants viewed tool stimuli rendered invisible by interocular suppression (Fang and He, 2005, Tettamanti et al., 2017), a method in which each eye receives different visual input. The specific method employed in these studies was Continuous Flash Suppression (CFS), which shows a dynamically flashing and highly salient mask to one eye, such that conscious perception of a low-contrast stimulus shown to the other eye is disrupted. In line with lesion patient DF, dorsal content could be processed and affected participants' behaviour without reaching conscious perception. Yet several studies found no such dissociation with similar suppression techniques (Fogelson et al., 2014, Hesselmann and Malach, 2011). Even patient DF's accurate hand opening during grasping has been criticised as relying on haptic feedback rather than unconscious dorsal visual processing (Schenk, 2012). Reasons for these diverging patterns of results have remained unclear. Arguably, suppression techniques may have been too dissimilar between studies, allowing for residual liminal conscious perception to reach participants' higher visual cortices in some instances (Hesselmann et al., 2018).

Recently, a further study tackled this topic in a more nuanced manner. Utilising the above-mentioned method, CFS, Ludwig et al. (2016) modulated object perception parametrically, rather than dichotomously. With six different mask contrasts, they examined the relationship between stimulus information, as correlated with subjective awareness, and neural activity across a broad range of visibility. As expected, ventral activity displayed a linear dependency on mask contrast. Dorsal areas on the other hand revealed a non-linear relationship, which

resembled a step-like function. At a particular mask contrast, decoding accuracy, as an indirect measure of category-specific functional activity, dropped to chance performance (see figure 2). Though this finding did not match studies which had found intact dorsal processing without any awareness, these differences in the shape of the visibility response function (i.e. linear versus step-like) piqued our interest. Might there be an all-or-nothing principle in action-related visual perception, whereby liminal visual input is cut

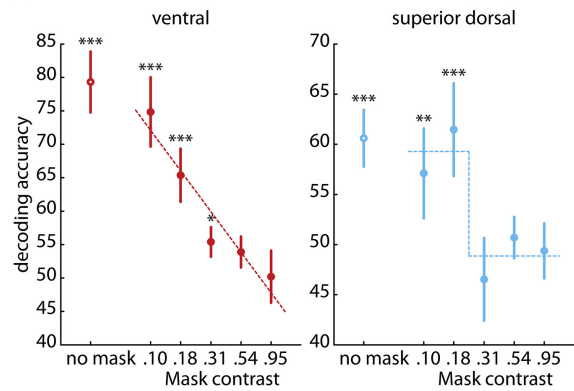


Figure 2. Linear and step-like models of stimulus signal (e.g. mask contrast) versus functional activity as observed by Ludwig et al. (2016).

off at a certain point? Could some studies have set their contrasts just beyond this cut-off point, whereas others had used stimuli that failed to reach this threshold?

To answer these questions, we designed a further study with a parametrical approach regarding stimulus information. However, rather than using interocular suppression, we decided to explore an alternative method of stimulus degradation. While highly effective at disrupting awareness, interocular suppression is unlikely to arise in the natural world. More commonly, everyday objects are binocularly viewed in noisy settings, e.g. in bad lighting, partially obstructed or for short durations. Still, human capacity for object recognition and action adaptation in dynamic situations remains remarkably robust.

In this functional magnetic resonance imaging (fMRI) study, we employed a more natural viewing paradigm and used visual noise to modulate stimulus information and obtain a distribution of subjective and objective recognisability, focusing on the threshold of awareness. We aimed to compare functional representations of stimulus categories in the two pathways across the visibility scale, from pure noise to fully recognisable object. In the following text, unless otherwise specified, the word "visibility" denotes recognisability of an object in noise.

2. Methods

2.1 Participants & Setup

Twenty-one participants (14 females, mean age 25, range 20-32, 17 right-handed), recruited via a student mailing list, took part in the fMRI experiment. Following this first experiment, a subset of fourteen participants completed an additional psychophysical experiment with the

same procedure, except for an added category discrimination task. Before initiation, the study was approved by the ethics committee of the German Psychological Society (DGP). Participants were naïve to the purpose of the study and reported understanding the task. None fell asleep or showed signs of repeated non-response during the fMRI scanning session. Realignment parameters showed negligible movement in the scanner (max. displacement 5 mm, max. rotation 3.8°) for all participants. Hence, no participants were excluded.

We created the visual stimuli (see below) and both the experimental and analytical scripts using Matlab 7.9.0 (MathWorks Inc., Natick, MA). Stimuli were presented with The Psychophysics Toolbox (<http://psychtoolbox.org/>). In the behavioural experiment, images were shown on a 19" CRT screen with a resolution of 1280x960 and a refresh rate of 60 Hz, whereby participants placed their heads on a chinrest. Within the scanner, images were presented on a NordicNeuroLab 32" LCD-Monitor with a resolution of 1024x768 pixels and an image refresh rate of 120 Hz. Viewing distance from the eyes to the screen was 154 cm within the fMRI scanner. Thus, each pixel subtended roughly 0.012° of visual angle.

We acquired functional data via T2*-weighted gradient-echo echo-planar imaging on a 3T MRI scanner (Tim Trio, Siemens, Erlangen), recording 214 volumes in each of the six runs. Anatomical images were acquired using a T1-weighted MPRAGE sequence.

2.2 *Stimuli*

We chose our stimuli with the goal of targeting the two pathways, while controlling for possible confounds. Face and tool stimuli were the most obvious and well-tested categories, though the variance of shape (i.e. oval faces versus elongated tools) was a potential confound. Therefore, we balanced the typically elongated tool stimuli with non-elongated manipulable objects. Altogether, we collected thirty grayscale stimuli from prior sets used in our lab. They consisted of ten faces, ten elongated and ten non-elongated manipulable objects. To balance the number of exemplars per category, face stimuli were doubled. A second potential confound were low-level image statistics, such as contrast and luminance.

To start from a balanced baseline before applying noise, all thirty stimuli underwent low-pass 2D Gaussian filtering, and matching with the SHINE toolbox (see figure 3).



Figure 3. Original thirty stimulus exemplars. They include ten faces, ten elongated and ten non-elongated manipulable objects are shown after low-level adjustment with the SHINE toolbox. These images without noise were shown to participants once prior to the experiment to ensure recognition of object identity.

In order to generate a spectrum of object information available to the viewer, we then applied visual noise to our stimulus images. Beyond manipulating contrast and introducing noise on top of an image, one can use Fourier transformations to manipulate image statistics more delicately. We chose to adapt a method employed by Roth and Zohary (2015), and first Fourier-transformed our thirty images to extract each individual phase spectrum. As demonstrated by Piotrowski and Campbell (1982), this image statistic most determines recognition of natural images. We then generated five noise images per original image with an amplitude spectrum of $1/f$ and extracted their phase spectra, too. This type of noise, also called “pink noise”, is customary for natural images, e.g. scenes in nature. The power spectrum of an image is the second piece of information gained from a Fourier transformation. The total power spectrum determines image contrast, and thus variations can compromise low-level image statistics. Therefore, we calculated an average power spectrum across all thirty images. We then inversely transformed the original image phase spectra and the pink noise phase spectra together with the overall average power spectrum. To create a distribution of stimulus information, signal-to-noise ratios (SNRs) were set at six logarithmically spaced intervals between 10% and 30% (image-to-noise). These ratios were found to target the threshold of recognisability in a brief behavioural piloting experiment ($N=7$).

We decided on a high number of visibility levels to catch artefacts within linearity that might suggest a non-linear function due to a shortage of data points. We added one condition of pure noise (no signal) and one highly visible ratio at 75%, thus yielding eight noise ratios.

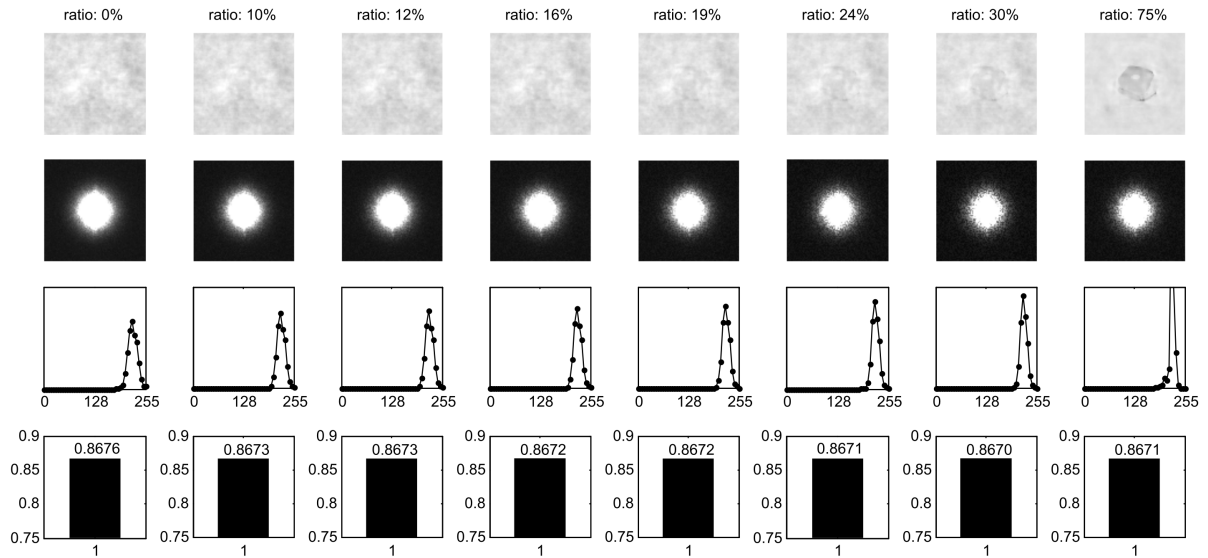


Figure 4. Noise image properties. Sample set of the noisy images at eight visibility levels, with signal-to-noise ratios ranging from 0% to 75%. In between, there were six logarithmically spaced intervals to target the threshold of object recognition (10-30%). The three rows below display a few important image statistics. In order, they are the Fourier amplitude spectra, luminance histograms and root mean square (RMS) contrast.

Luminance histograms, root mean square contrasts and Fourier amplitude spectrums across noise levels were similar or almost identical, due to magnitude averaging (see figure 4). We used five different noise images for each of the 30+10 stimuli (20 tools, 10 faces + 10 faces) at eight image noise ratios to create 1600 images prior to the experiment. They were accessed via a fresh randomization matrix for each subject.

2.3 Procedure

After a short introduction acquainting participants with the stimuli and ensuring comprehension of the task and awareness scale (see Fig. 5A), participants were tested on object recognition. They obtained printed examples of all thirty stimulus exemplars and were asked to simulate using the manipulable objects or to identify an individual's gender.

In the main experiment, there were six runs, which consisted of 64 trials and lasted approximately eight minutes each. During the trial, participants were shown the stimulus image for one second. After a jitter (i.e. variable delay) of 1-3 seconds they were asked to give a perceptual awareness scale (PAS) response within 1.5 seconds. In their right hand, participants held a response console with four keys in a row, which corresponded to their four fingers (excluding the thumb) and mirrored the four circles shown on the response screen. Pressing one of the keys changed the circle to an 'x' to confirm response registration. The next trial started

after a jitter of 2-4 seconds. The procedure of the trials is visualized in figure 5B. Altogether, the duration of scanning in the main experiment lasted roughly 60 minutes.

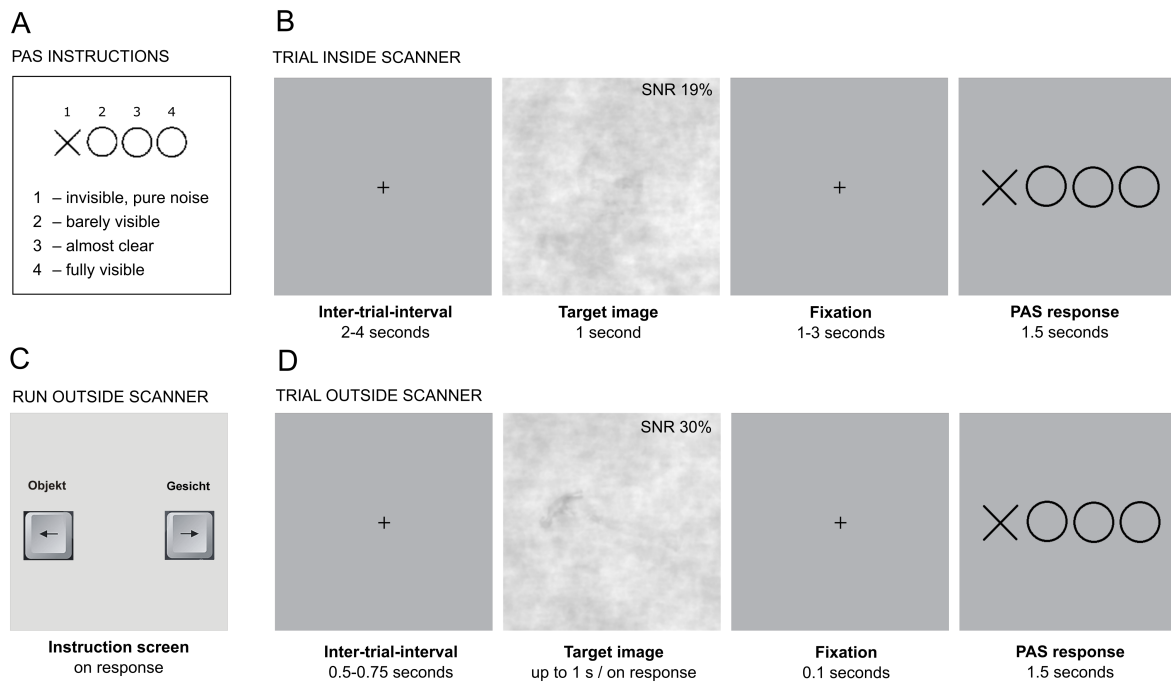


Figure 5. Procedure. Stimulus images in panels B and D are examples, shown here with their SNR. A) Instructions for subjective ratings on the perceptual awareness scale. B) Trial procedure inside scanner. After a variable delay of 2-4s, the target stimulus was shown for one second. Following another variable delay of 1-3s, four circles appeared, mirroring participants' response buttons in their right hand. On button press, the corresponding circle turned to a cross. The response screen was shown for up to 1.5 seconds. C) Instruction screen shown to participants before each run in the behavioural experiment, persisting until participants pressed a button to initiate the run. Here, the left arrow corresponded to "object", while the right arrow denoted the "face" category. Directions were balanced among participants. D) Trial procedure outside the scanner. Constructed to approximate the fMRI experiment, this procedure included an additional task while the stimulus image was presented: participants were told to categorise the stimulus.

All fourteen participants who agreed to the psychophysical experiment had previously attended the fMRI experiment. Though constructed to approximate the original fMRI session, this new experiment included one crucial addition. Participants were presented with a randomly assigned instruction screen at the start of each run, outlining the association of arrow keys with category, e.g. "right" for "object" and "left" for "face" (see figure 4C). Rather than passively viewing the stimulus at the beginning of each trial, participants were instructed to categorize the object as a tool or a face in advance of the perceptual awareness rating (see trial procedure in figure 5D). As before, there were six runs of 64 trials. Since participants could reduce presentation durations by giving responses, the psychophysical experiment was shorter and lasted roughly 30 minutes.

2.4 Analysis

2.4.1 Behavioural analysis

To analyse participants' behavioural measures, we averaged responses given during the psychophysical and fMRI experiments across participants and plotted them at each visibility level. We also report the standard error of the mean (SEM), denoted by the use of “±”. As stated above, objective responses (discrimination performance) were collected only in the psychophysical experiment. In the plots, the lowest and highest visibility levels stand apart from the other data points, since they are not part of the logarithmic scale. Furthermore, the lowest level contained no signal, such that categorisation was based solely on a pre-assigned category within the code of the noise procedure outlined above. This prior allocation was used to approximate a baseline at which one would expect chance performance.

Since we aimed to compare perceived stimulus information and functional processing between the two pathways, it was essential to show a strong correlation of our physical measure of stimulus signal (i.e. visibility level or SNR) with subjective awareness (i.e. PAS ratings). Therefore, we performed a correlation analysis of mean PAS per SNR and SNR alone. Using a Fisher transformation, we report this correlation coefficient, averaged across participants.

2.4.2 FMRI analysis

Preprocessing, including realignment, slice-timing, coregistering the images to anatomical scans and smoothing with 4 mm full width at half-maximum (FWHM) isotropic Gaussian kernels was performed in SPM 12 (<http://www.fil.ion.ucl.ac.uk/spm>) within Matlab (MathWorks Inc., Natick, MA). In each condition, activation was quantified via a general linear model (GLM) with the haemodynamic response basis function in a block design. It contained sixteen regressors (two stimulus categories at eight visibility levels) and six realignment parameters in both univariate and multivariate analyses.

Regarding our regions of interest (ROIs), we decided on a partially data-driven approach. We decoded accuracy-minus-chance maps at the highest visibility level for each participant. Subsequently, we performed spatial smoothing with a 6 mm Gaussian kernel and normalised the maps to MNI space. Via group analysis we estimated a statistical parametric map (SPM) across participants, which retained the freedom of setting the activation threshold. We then combined these statistical maps with anatomical probability maps from “The Anatomy Toolbox” (Eickhoff et al., 2005) using Marsbar (<http://marsbar.sourceforge.net/>). At the default SPM threshold setting, namely family-wise error (FWE) 0.05, ventral regions in the posterior fusiform gyrus showed sufficiently strong activation, while some dorsal areas were left with

single digit voxel counts. Thus, we used a more liberal, uncorrected threshold of 0.0001 for the SPM maps in dorsal ROIs and combined them with the probability maps from the toolbox. For both univariate and multivariate analyses, ROIs were transformed into participants' native space. ROIs are rendered in figure 8B.

Univariate analysis of the data was performed with averaged parameter estimates, which quantify mean activation within a defined ROI. The mean beta value was calculated across runs and then group-wise per visibility level and for each category in the associated cortical regions, i.e. faces in ventral and tools in dorsal areas.

We conducted multivariate pattern analysis (MVPA) in participants' native space in each ROI in a leave-one-run-out cross-classification approach for tools versus faces using a linear support vector machine with The Decoding Toolbox (Hebart et al., 2014). This kind of analysis is suited to decode more distributed information, rather than large-scale, homogenous activity. Even without strong mean activation and regardless of positive or negative directionality, it remains sensitive to task-relevant patterns of activity (Haynes and Rees, 2006). We performed two further MVPA analyses. In the first, we investigated differences between the left and right hemispheres by splitting our regions of interest along the midline. The other required restructuring of conditions at the level of our GLM, in order to sort our conditions based on behavioural responses (PAS ratings) rather than predefined stimulus signal (SNR). In this analysis, we attempted a more direct examination of functional processing as related to stimulus awareness.

2.4.3 Statistical analysis

We tested for linearity across visibility levels 2-7, as level 1 and 8 were not on the logarithmic scale but rather floor and ceiling values. We performed standard repeated-measures analyses of variance (rm-ANOVA) in SPSS (IBM Corp. Released 2015. IBM SPSS Statistics for Windows, Version 23.0. Armonk, NY).

We added a Bayes factor analysis to characterise the relationship between stimulus signal and functional activity in the main MVPA analysis. Bayesian analysis computes probabilities of various competing hypotheses, based on prior knowledge. These odds are described by the Bayes Factor (BF), with any value above 1 supporting the hypothesis, while lower values point towards the null or a competing hypothesis. In general, BF above 3 are considered "substantial evidence", BF higher than 10 are "strong" and values over 100 are "decisive" (Kass, 1995). In this case, we aimed to compare two models of brain activity in relation to visibility level. We tested for a linear as well as a non-linear, or more specifically, step-like model, as in the study

outlined in the introduction (Ludwig et al., 2016). The linear model was formulated as “accuracy \sim level + participant”, while the non-linear model was formulated as “accuracy \sim step + participant”. The values of the level vector corresponded to the six logarithmically scaled SNRs ranging from 10% to 30%. We set the value of the step vector at the largest increase in decoding accuracy across all six levels. Each model was compared to the null model, resulting in a BF_L (linear) and a BF_S (step). Finally, simply by dividing competing models, we calculated a linear-versus-step-like Bayes factor (BF_{LS}). Results > 1 therefore indicate that the data are more consistent with the linear model as compared with the step-like model. We performed these calculations using the BayesFactor package version 0.9.12-2 by Morey (2015) in R (Version 3.3.2; www.r-project.org; R-Studio Version 1.0.136; www.rstudio.com) with the factor “participant” as random effect.

To increase readability, statistical results within this manuscript are reported as p-values only. Full statistical details can be found in the published journal article (Darcy et al., 2019).

3. Results

3.1 Behavioural results

3.1.1 Subjective

During the experiment, we asked participants to rate their awareness of the objects and faces in noise. Overall, stimulus signal had a considerable effect on subjective ratings, regardless of object category and in both experimental settings ($p < .001$ both inside and outside the scanner, see figure 6A-B). Linearity was also observed inside and outside the scanner (both $p < .001$). Subjective ratings cover a comparable range in both behavioural and functional experiments across the visibility spectrum. The ceiling and floor values showed consistent minimum and maximum ratings at the lowest and highest visibility levels respectively, with an average of 1.29 (SEM \pm 0.05) and 3.79 (\pm 0.05) outside the scanner and 1.12 (\pm 0.02) and 3.82 (\pm 0.04) inside the scanner. In a direct rm-ANOVA, we observed slightly higher overall subjective visibility ratings in the psychophysical setting (mean: 2.08), compared with the fMRI setting (mean: 1.89; $p = .05$). Both PAS measures and statistical results were similar for each category, though faces were rated more visible than tools in the logarithmically spaced levels of 2-7 in both experiments. On average, ratings for faces were 0.53 (\pm 0.04) higher inside and 0.51 (\pm 0.04) higher outside the scanner.

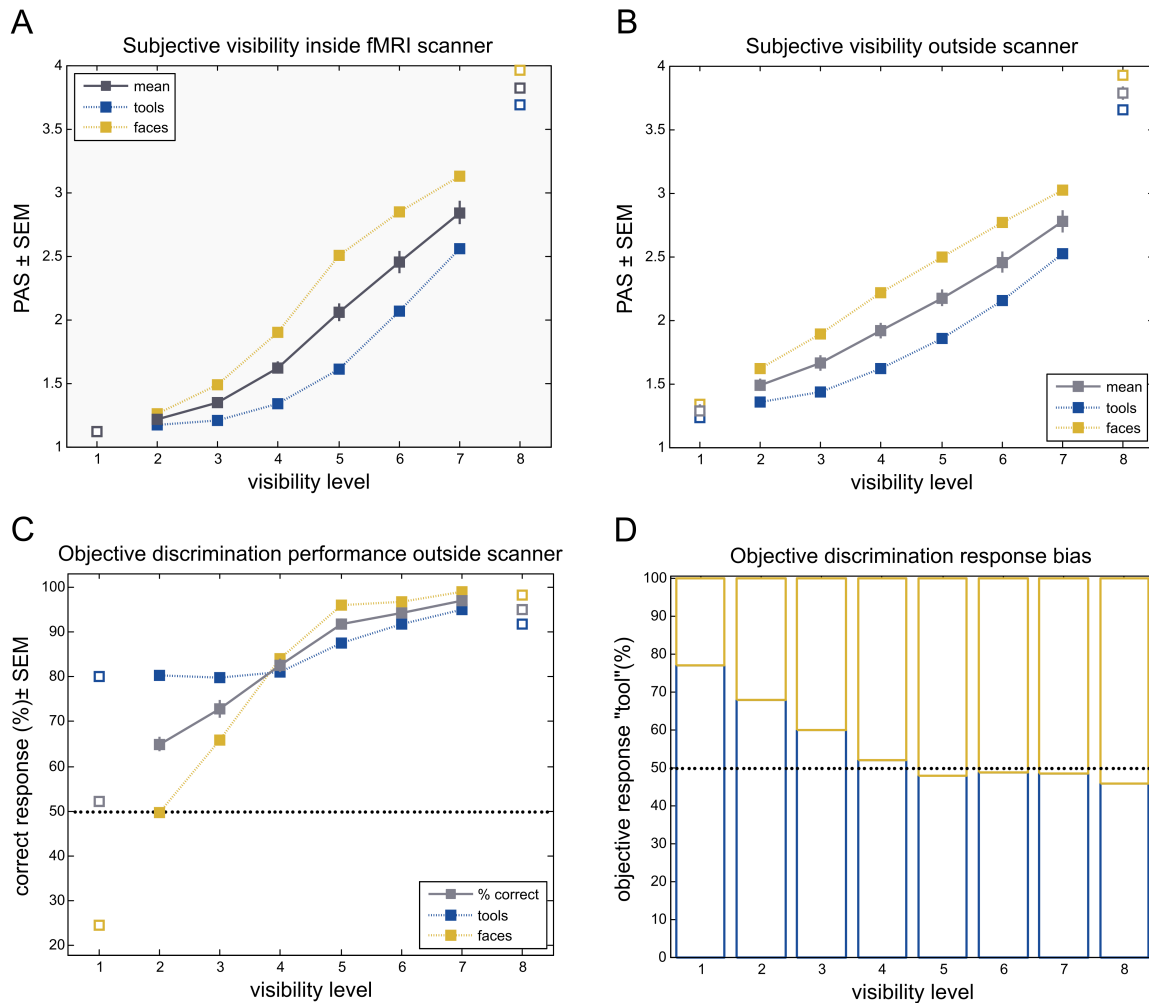


Figure 6. Behavioural results (N=21) of fMRI (panel A) and behavioural experiments (panels B-D). Mean results are plotted for each visibility with standard error of the mean (SEM) bars. Ceiling (level 8, 75% SNR) and floor (level 1, 0% SNR) values are separated from the logarithmically spaced values in between. Additionally, the results are split into image categories tools (blue) and faces (yellow). A) Subjective visibility in the main fMRI experiment, as measured by the perceptual awareness scale (PAS) of 1-4. B) Analogously plotted subjective visibility in the behavioural experiment outside the scanner. C) Objective discrimination performance, as a percentage of correct responses plotted against visibility level. Data points at 0% SNR are outlined, because their category was randomly assigned. D) Proportion of responses given to each category at each visibility level, excluding non-responses (blue = tool, face = yellow). These were plotted to investigate the divergence of discrimination performance at low visibility levels.

3.1.2 Objective

In the behavioural experiment, we asked participants to give a discrimination response regarding stimulus category (i.e. “face” or “tool”). As for subjective ratings, objective discrimination performance was also modulated by the factor “signal” ($p < .001$), and showed a significant linear trend, increasing with stimulus signal ($p < .001$, see figure 6C). At zero percent signal, category discrimination approximated chance level (52.2%). As outlined above (2.4.1), these stimuli contained no signal, such that categorisation could be neither correct nor incorrect. Still, we report these results according to prior allocation during the noise procedure. At the

next level (SNR 10%), though participants had rated stimuli between “barely visible” and “invisible (mean PAS = 1.49), their performance reached significance (65%, $p < .001$). From the fifth level (SNR 19%) onwards, discrimination performance was reliably above 90%.

When split into the two stimulus categories, the discrimination task presented an unanticipated finding. There appeared to be a considerable bias towards tool categorization at lower visibility levels. At 0% signal (pure noise), 77% of stimulus images were categorised as tools (figure 6D). To quantify category discrimination bias according to signal detection theory, we estimated the sensitivity index d' and the decision criterion C . Arbitrarily, we defined tool stimuli as “signal present”, and face

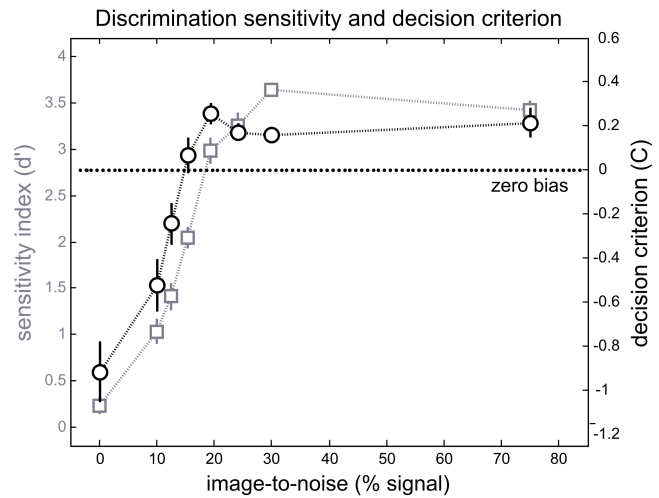


Figure 7. Discrimination response bias. Sensitivity index d' (grey) and decision criterion C (black, in units of standard deviation from zero bias reference line) plotted per SNR. Since category “tool” was arbitrarily defined as “signal present”, values of $C < 0$ indicate a bias towards a “yes” response, i.e. tool categorisation.

stimuli as “signal not present”. Then we subtracted Z-scores of false alarms (tool categorisation of a face) from the Z-scores of hit rates (tool categorisation of a tool) at each visibility level. Figure 7 plots sensitivity index d' and decision criterion C relative to the zero bias location per SNR. At low visibility levels, discrimination sensitivity (d') decreases. Calculated relative to the zero bias location in units of standard deviation, decision criterion C displays a similar shape. In this case, negative values point towards a “yes” response, i.e. categorisation of a stimulus image as “tool”. As seen in the figure, lower signal levels biased participants towards the response “tool” by roughly one unit of standard deviation.

3.2 FMRI results

3.2.1 Main multivariate pattern analysis

Mean results of multivariate pattern analysis for faces versus tools are plotted in figure 8. Chance-performance of the classifier is at 50% decodability, since there were two categories. At visibility levels one (0% SNR) and two (10% SNR), decoding accuracies were roughly at chance in both pathways (range 47.9% - 50.3%). At higher levels, both ventral and dorsal decoding accuracies increased. A notable difference concerned maximum decoding accuracies.

While the ventral region reached ceiling decoding accuracies of roughly 80% (max. 81.2%, level 8), the strongest results in dorsal ROIs, though significantly above chance, remained around 60%. At the highest SNR, intraparietal sulcus showed 61.0% (± 2.79 SEM) decodability and superior parietal cortex reached 61.2% (± 2.52 SEM). Maximal mean decoding accuracy in inferior parietal cortex was at 62.7% (± 1.25 SEM) at visibility level 7.

Classical statistics confirmed significant effects of signal on decodability in all ROIs and strongly favoured linearity. Apart from IPS, where results were nonetheless significant ($p = .005$), p -values were below 0.001 in all regions of interest.

We added a Bayesian analysis to quantify probabilities of various models of the decodability function as related to stimulus signal (for details of the procedure, see 2.4.3). Both the linear

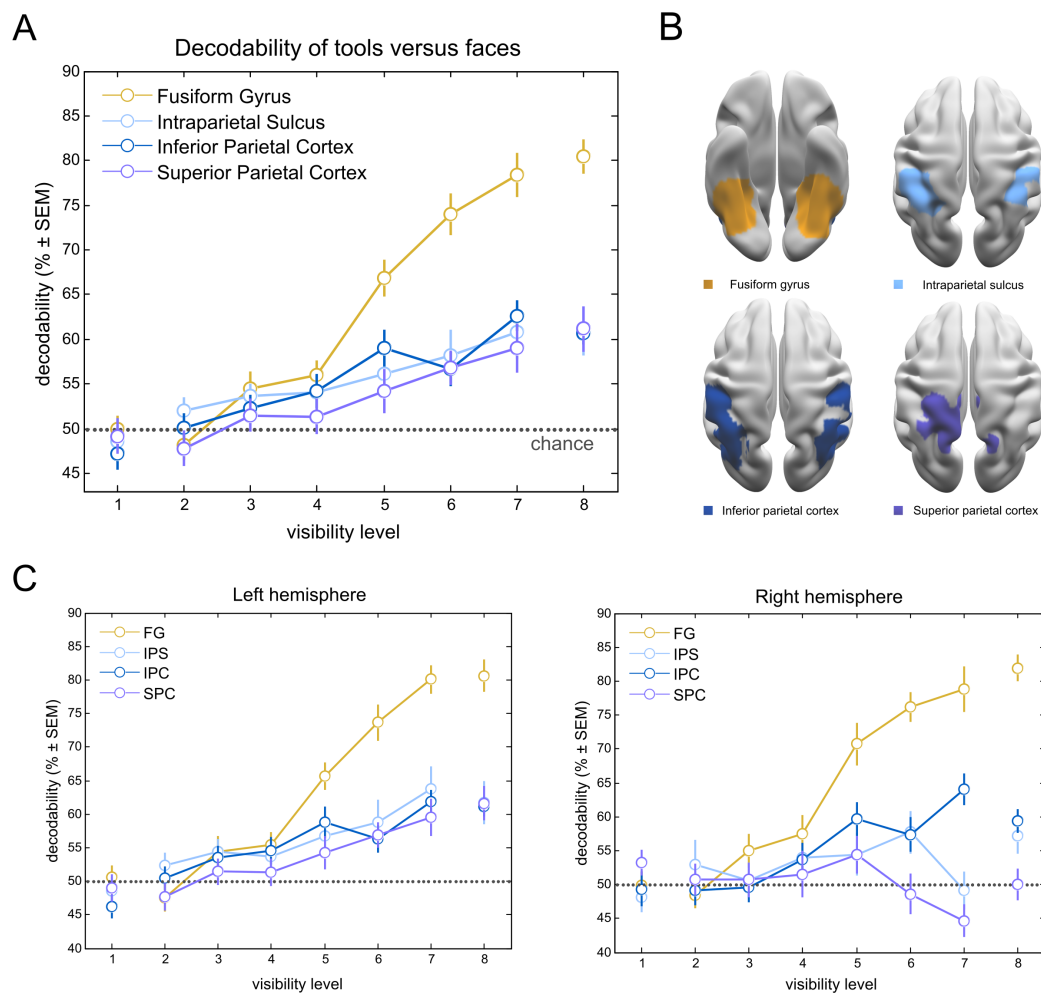


Figure 8. Decoding results (N=21). Mean decodability of tools versus faces plotted for each visibility level (1-8) with bars denoting standard error of the mean (SEM). Chance performance is at 50%, since there were two image categories. Fusiform gyrus is depicted in yellow, while dorsal ROIs are coloured light blue (intraparietal sulcus), blue (inferior parietal cortex) and purple (superior parietal cortex). A) Overall decoding results in both hemispheres. B) ROIs projected on ventral (FG) and dorsal views (IPS, IPC, SPC) of flattened surface maps of the brain. C) Decodability in left and right hemispheres. In right SPC, N=20.

BF /null (BF_L) and linear BF / step-like BF (BF_{LS}) showed evidence for linearity as the most likely hypothesis in all regions. The strongest results were obtained in fusiform gyrus, where BF_L over 100 supported a linear over a null hypothesis. With the step set between visibility levels 4 and 5, a further decisive result ($BF_{LS} > 100$) also favoured a linear over a step-like shape. The same trend was observed in dorsal ROIs. Linearity over a null hypothesis was favoured decisively ($BF > 100$) in IPS and IPC, with SPC showing substantial evidence ($BF_L = 23$). With the largest increments between levels 2 and 3 (IPS, IPC) or 6 and 7 (SPC), Bayes factors supported a linear over a step-like model in all three dorsal ROIs (IPS = 9, IPC > 100, SPC = 96).

3.2.2 Hemispheric analysis

Using Marsbar (<http://marsbar.sourceforge.net/>) to split regions of interest along the midline, category-selective regions of interest could be defined in both hemispheres, with the sole exception of superior parietal cortex in one subject. Their superior PC was empty and thus not included in this analysis. As depicted in figure 8C, results in each of the hemispheres were quite similar in all ROIs, apart from SPC. Here, results differed strongly, with 61% decoding accuracy in left superior parietal cortex versus a chance performance of 50% in right SPC ($t(19) = 5.04$, $p < 0.001$) at visibility level 8. The most likely explanation for this discrepancy is the size of SPC in the right hemisphere. The mean number of voxels across participants was 6 (SD = 2), which would have resulted in highly noisy data. As outlined in the analysis section (2.4.2), ROIs were combinations of anatomically defined functional probability maps and group-level activity for stimuli at the highest signal level. Left superior PC was far larger than its counterpart, at a mean of 190 voxels. As previous studies have described category specific dorsal regions as left-lateralised (Brandi et al., 2014), ROI asymmetry in this experiment was in line with the literature.

3.2.3 Univariate analysis

Mean beta values at each visibility level are plotted in figure 9. Results were estimated for face stimuli in ventral regions and tool stimuli in dorsal regions. There was a clear upward trend in both ventral and dorsal ROIs across the visibility spectrum. Repeated-measures ANOVA results showed significant effects of signal on beta values and strongly favoured linearity in all ROIs but IPC. Both an effect of signal and a linear relationship with visibility level were highly significant in FG and IPS ($p \leq 0.001$ in all cases), demonstrable in in SPC ($p \leq 0.016$), but not significant in IPC ($p_{\text{effect}} = 0.83$, $p_{\text{linear}} = 0.71$).

Compared to MVPA results, univariate data show a notable discrepancy in inferior parietal cortex (IPC). In this region, SNR had no effect on parameter estimates. Univariate analysis is most sensitive to large-scale, ideally homogenous activity across a certain region, since mean activity gives rise to the parameter estimate. IPC, the largest dorsal ROI in this experiment, contained 665 voxels on average, whereas the other two dorsal ROIs, intraparietal sulcus (IPS) and superior parietal cortex (SPC) consisted of only 228 and 195 voxels. If a substantial number of voxels within IPC were not involved in category processing, these inactive voxels would have lowered the mean parameter estimate. Results of multivariate analyses on the other hand, are not diminished by these “inactive” voxels. MVPA is capable of decoding more distributed activity and retaining sensitivity to task-related patterns, regardless of mean activation or positive or negative directionality (Mur et al., 2009, Haynes and Rees, 2006). Therefore, it is better suited to reveal “distributed multidimensional effects” of functional brain activity (Davis et al., 2014, Kriegeskorte et al., 2006, Jimura and Poldrack, 2012, Friston, 2009).

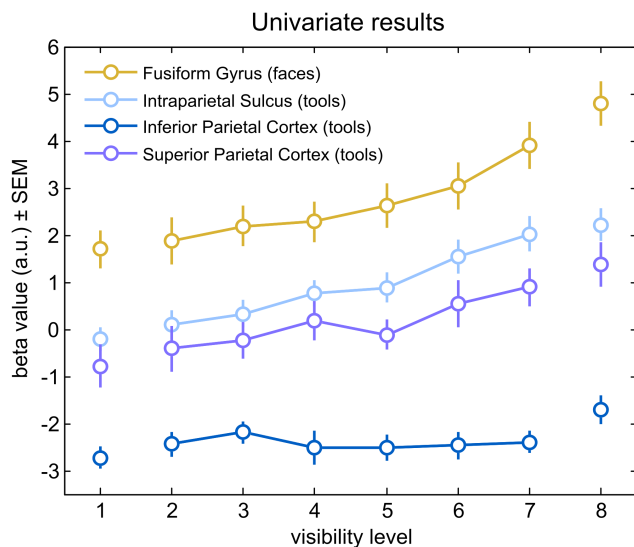


Figure 9. Univariate results (N=21). Average beta values in arbitrary units obtained for each ROI for its associated category (see brackets) plotted per visibility level. Yellow depicts the ventral region of interest, fusiform gyrus. Dorsal ROIs are intraparietal sulcus (light blue), inferior (dark blue) and superior parietal cortex (purple). Error bars plot standard error of the mean (SEM).

3.2.5 Awareness analysis

In this study, our goal was to characterise the relationship between the visual perception of noisy stimuli and functional activity in the two pathways. Yet, the results we presented so far were plotted against visibility level, rather than direct measures of awareness. In this section, we provide our reasoning for this choice.

As stated above (2.4.1), this study was based on noisy objects intended to target a spectrum of visibility around the threshold of awareness. It was therefore paramount that subjective ratings of awareness and visibility level (i.e. stimulus signal) were highly correlated. To quantify this

link, we performed a correlation analysis. The mean Fisher-transformed correlation coefficient comparing subjective visibility ratings (PAS) at each SNR and SNR alone was 99.15 % (± 0.13), indicating a strong correlation.

Nonetheless, given that we collected subjective measures of awareness during the experiment, a direct analysis without predefined measures of stimulus information (SNR) may also be of interest. We did indeed perform this analysis and additionally quantified the distribution of PAS ratings given by participants during the fMRI experiment (see figure 10). Three participants could not be included due to a lack of trials in some conditions and therefore insufficient viable runs (3 out of 6). All remaining participants (N=18) retained at least five runs for the analysis.

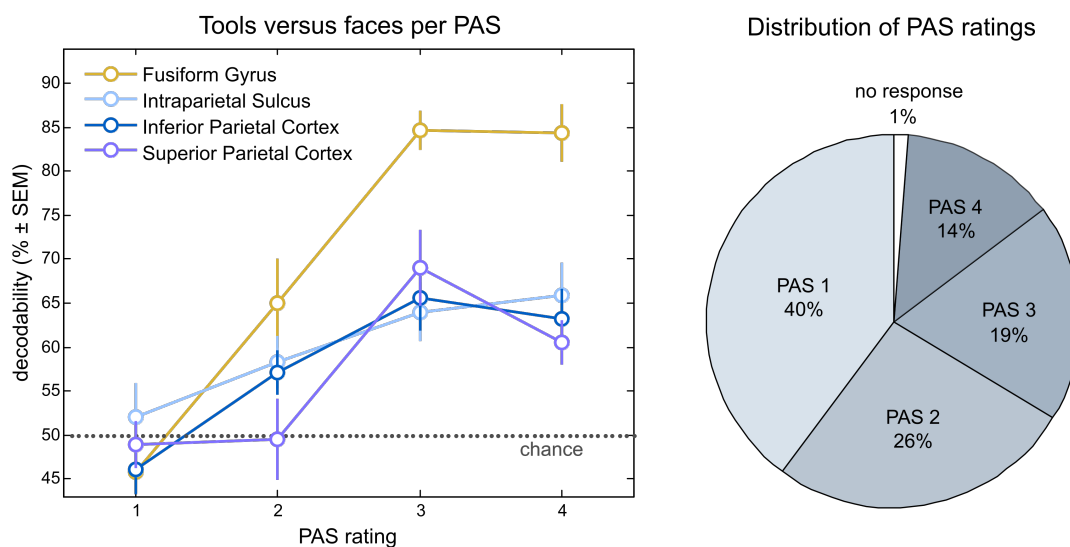


Figure 10. Decodability of tools versus faces per PAS rating and overall distribution of ratings (N = 18). Yellow depicts the ventral region of interest, fusiform gyrus. Dorsal ROIs are intraparietal sulcus (light blue), inferior (blue) and superior parietal cortex (purple). Error bars plot standard error of the mean (SEM). The percentages in the pie chart of PAS ratings relate to the proportion of ratings given during the whole fMRI experiment (one response per trial), averaged across participants. Non-responses occurred when participants did not respond within the allotted time frame (1.5 seconds).

As expected from the robust correlation result above, the results demonstrated a clear increase of decodability with higher PAS ratings in all ROIs. Most regions clearly exceeded chance decodability (50%) at PAS rating 2 (“barely visible”), with the exception of superior parietal cortex, which reached robust decoding accuracy at a rating of 3 (“almost clear”). Interestingly, at the highest PAS rating, both IPC and particularly SPC revealed a drop in decoding accuracy. Performed analogously to those in the main experiment, ANOVAs confirmed statistical effect of awareness rating and linearity in all cases ($p \leq .001$ in all regions but IPS, where $p \leq .022$).

This result demonstrated that category processing showed a linear dependency in both pathways, even as a direct function of awareness.

However, since the interesting part of this function was contained within a narrow window at the threshold of object recognition, we argue that behavioural ratings of awareness are insufficient, particularly since there were only four. Furthermore, subjective intervals between ratings were likely somewhat distributed, as evidenced by the large standard errors of the mean at the two intermediate ratings. A far more detailed awareness rating task would be required and likely overwhelm participants. In addition, an analysis with unequal numbers of ratings is not balanced (see figure 10) and therefore more susceptible to noise. For these reasons, we concluded that assessing the shape of this function was not sufficiently reliable and therefore reported our results in relation to stimulus signal, rather than awareness ratings.

4. Discussion

4.1 Summary of results

We successfully modulated both subjective awareness and discrimination accuracy of visually presented object categories by applying visual noise. Functional data of twenty-one participants who viewed these stimuli, demonstrated a linear correlation between signal-to-noise-ratio and decoding accuracy in both visual pathways. Both classical and Bayesian statistical analysis verified this relationship. As one might expect, the noisier the stimulus, the weaker the associated functional activity in the brain. We confirmed this pattern of results both in a univariate analysis and in hemispheric multivariate analyses. The sole exception, the superior dorsal region in the right hemisphere, was composed of too few voxels to be considered reliable. Further, the linear relationship to functional activity persisted in direct correlation with awareness ratings, rather than stimulus information.

4.2 Relation to previous findings

This study cannot confirm prior work that found behavioural differences or extant dorsal brain activity even though participants were unaware of seeing objects (Fang and He, 2005, Tettamanti et al., 2017). We found neither preserved activity, nor a step-like reduction at a certain noise level (Ludwig et al., 2016). However, there are important methodological distinctions, particularly regarding suppression technique, that could provide an explanation for deviating results. The studies mentioned above used interocular rivalry, which might allow

visual information presented to one eye to extend into higher visual cortices without conscious perception. This could not occur with application of visual noise to binocularly viewed images. It is therefore possible that the persistence of dorsal processing is contingent on this specific suppression method. However, even within this field, results are inconsistent (Hesselmann and Malach, 2011, Ludwig et al., 2015, Fogelson et al., 2014). Future studies, perhaps using further methods of stimulus degradation, will need to address this matter.

A recent study by Binder et al. (2017) observed an unanticipated finding regarding dorsal activity at higher levels of stimulus information. In their event-related fMRI study, it appeared that activity was highest not when stimuli were most recognisable, but at intermediate levels. In the present study, a similar pattern emerges in our analysis of activity dependent on perceptual awareness ratings in both IPS and SPC (figure 9). The theory examined by the above-mentioned authors was the “Level-of-Processing hypothesis” proposed by Windey et al. (2013). It describes a transition of awareness type along the visual hierarchy, ranging from parametrically distributed awareness of low-level visual features (e.g. colour) to an all-or-nothing principle of visual awareness for high-level features (e.g. enumeration). Testing whether these differences in awareness were reflected in activity, they found the highest levels of activity at intermediate PAS ratings in areas involved in conscious visual processing, which included fronto-parietal and insular regions. These “NCC ROIs” (neural correlates of consciousness, NCC), they suggested, might be related to attentional resources recruited due to task difficulty, which were not required for invisible nor highly visible stimuli. This establishes a link between attentional control networks and conscious visual perception (Corbetta and Shulman, 2002), perhaps modulated by expectations (Melloni et al., 2011) and task affordances (Bracci et al., 2017).

Undoubtedly, the dissociation of perceptual processing and “prerequisites and consequences” (Aru et al., 2012) of NCC remains challenging, particularly when consciousness research is dependent on participants’ report of percept.

4.3 Secondary observations and limitations

A notable result in our behavioural data regarded category discrimination performance in the behavioural experiment, which surpassed chance performance at the lowest level containing any signal (level two, SNR 10%, see figure 5). Both PAS ratings (mean: 1.49; halfway between “pure noise” and “barely visible”) and decoding accuracies (mean: 49.44 %) did not indicate category-related perception nor activity. In search of an explanation, one hypothesis rested on

generally higher subjective awareness of faces (mean: +0.52) and the tool bias observed in the discrimination task (see figure 6). Possibly, very weak impressions of faces resulted in correct identification in some instances, even at low visibility levels. In the others, participants were prone to select the tool category, even when they did not see anything. This could lead to an above-average performance. To correct for this discrepancy, one would require an adjustment to the signal-to-noise-ratios of faces to match those of tool stimuli. On the other hand, participants may be predisposed towards predicting that they possess comparatively stronger face recognition abilities. This assumption could offer an alternative explanation for the tool bias at low signal levels, but it does not clarify the strong categorisation performance at low signal levels.

A further observation pertained to the substantial discrepancy in peak decoding accuracies in the two pathways. As opposed to the ventral visual stream, targeting dorsal areas with two-dimensional images can prove a challenge. A photograph of a tool is not the ideal substrate to excite the dorsal visual system, which is typically implicated in visual processing related to real-world actions. Studies have shown that activity is altered and often stronger in parietal regions when objects are three-dimensional or when there are associated tasks such as reaching or grasping, even when these are only imagined (Freud et al., 2018, Cavina-Pratesi et al., 2007, Jeong and Xu, 2016, Fabbri et al., 2016). Without affordances for real action, activity in dorsal regions is likely not at full capacity. On the other hand, it might be difficult to compare the two streams adequately, if three dimensions and possibly real objects and actions are introduced. Practically speaking, experimental settings with real tools or faces within an fMRI scanner could prove rather challenging. Balancing experiments by requiring actions with ventrally processed objects would present its own difficulties and possibly alter activity patterns. Approaches gaining traction are augmented and virtual reality. In combination with imaging or electrophysiological technology, these methods could deliver highly realistic experimental setups within a confined space and offer exciting opportunities for vision research.

4.4 Connectivity and temporal dynamics

If higher-level dorsal activity is indeed unique in its relation to awareness, one would assume at least partial segregation from the ventral pathway, allowing functional autonomy. Yet increasingly, research on the two visual pathways is rejecting the hypothesis of functional independence. Rather, the two streams appear to interact and support each other in their respective capabilities. One of the originators of the two-streams hypothesis, David Milner,

recently reviewed examples of this process (Milner, 2017). He proposed that ventral processes could assist the dorsal system in complex visuomotor behaviour plans, while dorsal processing may support three-dimensional visual perception in ventral regions (see figure 11).

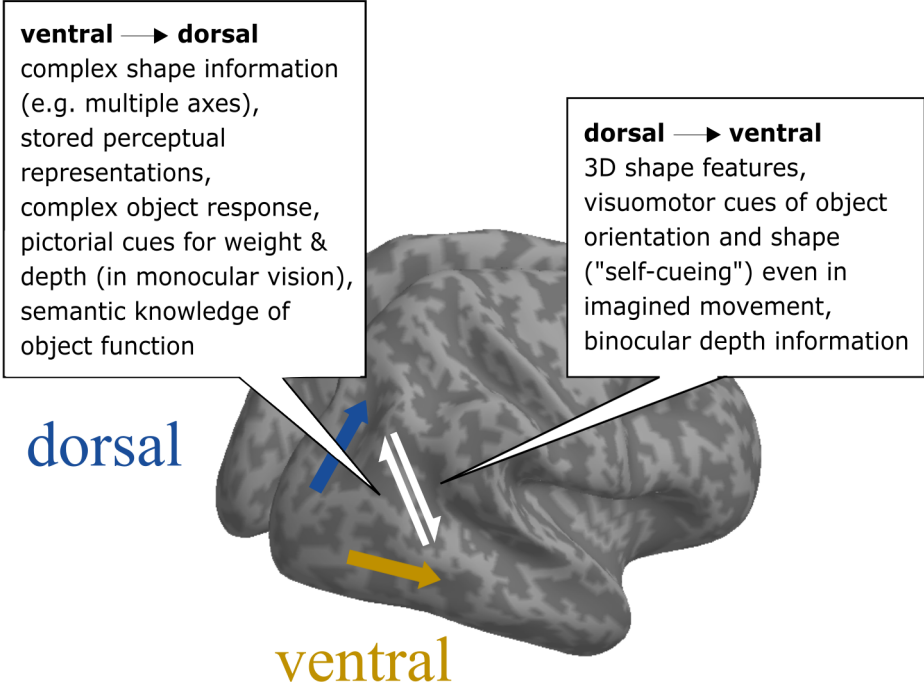


Figure 11. An updated version of the two-visual-streams hypothesis with a list of potential capacities for inter-stream interaction as outlined by David Milner (2017).

Reviewing functional and behavioural data of healthy subjects and neuropsychological evidence from patients, several authors have demonstrated these interactions (Schenk and McIntosh, 2010, Cloutman, 2013, van Polanen and Davare, 2015). Further important contributions emerge from anatomical data, e.g. histological studies on non-human primates or diffusion MRI in humans (Martinaud, 2017, Binkofski and Buxbaum, 2013, Budisavljevic et al., 2018, Felleman and Van Essen, 1991). Together with functional studies (Takemura et al., 2016, Rokem et al., 2017), these have shown extensive reciprocal connections between the two pathways at multiple levels.

A further dimension to consider is time, in which the two pathways likely play different but complementary roles, e.g. in upholding visual spatial constancy (Wu, 2014). A recent study by Erlikhman et al. (2016) used multivariate fMRI to investigate the construction of spatiotemporally dynamic object identities. Discussing patterns of activity found both in early motion-sensitive and higher-level parietal regions such as IPS, they argued that the visual pathways cooperate to integrate spatiotemporal object representations.

4.5 Updated theories and future considerations

The TVSH, as proposed thirty years ago, has been an important driver in the investigation of higher visual processing. Though one can no longer support a strict purpose-led divergence of visual processing, nor be certain that dorsal processing can operate in an isolated, non-conscious sphere, it remains highly influential. The observations of patients with apperceptive agnosia, such as DF, await further efforts to update our understanding of visual object processing.

As is often the case, the more a natural phenomenon is studied, the more complex it seems to become. To keep up, the general trend in biological and particularly neuroscience has moved towards computational modeling. The hope is that the gap between theory-based “top-down” science and empirical behavioural, functional and physiological data can be bridged.

Future studies on higher-level visual processing would do well to consider attentional and task-related affordances of stimulus objects, ideally incorporating activity due to attentional control networks in their models (Bracci et al., 2017, Bugatus et al., 2017). In differentiating and characterising subcomponents of the two visual streams, it would appear that sophisticated and possibly connectivity-attuned methods, e.g. MVPA, representational similarity analyses and dynamic causal modelling, are appropriate. Temporal characteristics and dynamics may be better characterised with electrophysiological methods that allow high temporal resolution, such as magneto- or electro-encephalography. Furthermore, transcortical magnetic or electrical stimulation can be applied to better infer causality by selectively disrupting cortical activity. Particularly regarding the dorsal stream, virtual reality may prove valuable in enabling three-dimensional, dynamic and possibly interactive experimental settings, thus bearing a much closer resemblance to the environment in which the human visual system developed.

References

- ARU, J., BACHMANN, T., SINGER, W. & MELLONI, L. 2012. Distilling the neural correlates of consciousness. *Neurosci Biobehav Rev*, 36, 737-46.
- BINDER, M., GOCIEWICZ, K., WINDEY, B., KOCULAK, M., FINC, K., NIKADON, J., DERDA, M. & CLEEREMANS, A. 2017. The levels of perceptual processing and the neural correlates of increasing subjective visibility. *Conscious Cogn*, 55, 106-125.
- BINKOFSKI, F. & BUXBAUM, L. J. 2013. Two action systems in the human brain. *Brain Lang*, 127, 222-9.
- BRACCI, S., DANIELS, N. & OP DE BEECK, H. 2017. Task Context Overrides Object- and Category-Related Representational Content in the Human Parietal Cortex. *Cereb Cortex*, 27, 310-321.
- BRANDI, M. L., WOHLSCHLAGER, A., SORG, C. & HERMSDORFER, J. 2014. The neural correlates of planning and executing actual tool use. *J Neurosci*, 34, 13183-94.
- BUDISAVLJEVIC, S., DELL'ACQUA, F. & CASTIELLO, U. 2018. Cross-talk connections underlying dorsal and ventral stream integration during hand actions. *Cortex*, 103, 224-239.
- BUGATUS, L., WEINER, K. S. & GRILL-SPECTOR, K. 2017. Task alters category representations in prefrontal but not high-level visual cortex. *Neuroimage*, 155, 437-449.
- CAVINA-PRATESI, C., GOODALE, M. A. & CULHAM, J. C. 2007. fMRI reveals a dissociation between grasping and perceiving the size of real 3D objects. *PLoS One*, 2, e424.
- CLASSEN, C. 1997. Foundations for an anthropology of the senses. *International Social Science*, 49, 401 - 412.
- CLOUTMAN, L. L. 2013. Interaction between dorsal and ventral processing streams: where, when and how? *Brain Lang*, 127, 251-63.
- CORBETTA, M. & SHULMAN, G. L. 2002. Control of goal-directed and stimulus-driven attention in the brain. *Nature Reviews Neuroscience*, 3, 201-215.
- CULHAM, J. C., DANCKERT, S. L., DESOUZA, J. F., GATI, J. S., MENON, R. S. & GOODALE, M. A. 2003. Visually guided grasping produces fMRI activation in dorsal but not ventral stream brain areas. *Experimental Brain Research*, 153, 180-189.
- DARCY, N., STERZER, P. & HESSELMANN, G. 2019. Category-selective processing in the two visual pathways as a function of stimulus degradation by noise. *Neuroimage*, 188, 785-793.
- DAVIS, T., LAROCQUE, K. F., MUMFORD, J. A., NORMAN, K. A., WAGNER, A. D. & POLDRACK, R. A. 2014. What do differences between multi-voxel and univariate analysis mean? How subject-, voxel-, and trial-level variance impact fMRI analysis. *Neuroimage*, 97, 271-83.
- EICKHOFF, S. B., STEPHAN, K. E., MOHLBERG, H., GREFKES, C., FINK, G. R., AMUNTS, K. & ZILLES, K. 2005. A new SPM toolbox for combining probabilistic cytoarchitectonic maps and functional imaging data. *Neuroimage*, 25, 1325-35.
- ERLIKHMAN, G., GURARIY, G., MRUCZEK, R. E. B. & CAPLOVITZ, G. P. 2016. The neural representation of objects formed through the spatiotemporal integration of visual transients. *Neuroimage*, 142, 67-78.
- FABBRI, S., STUBBS, K. M., CUSACK, R. & CULHAM, J. C. 2016. Disentangling Representations of Object and Grasp Properties in the Human Brain. *J Neurosci*, 36, 7648-62.
- FANG, F. & HE, S. 2005. Cortical responses to invisible objects in the human dorsal and ventral pathways. *Nature Neuroscience*, 10, 1380-1385.
- FELLEMAN, D. J. & VAN ESSEN, D. C. 1991. Distributed hierarchical processing in the primate cerebral cortex. *Cerebral Cortex*, 1, 1-47.
- FOGELSON, S. V., KOHLER, P. J., MILLER, K. J., GRANGER, R. & TSE, P. U. 2014. Unconscious neural processing differs with method used to render stimuli invisible. *Front Psychol*, 5, 601.
- FREUD, E., MACDONALD, S. N., CHEN, J., QUINLAN, D. J., GOODALE, M. A. & CULHAM, J. C. 2018. Getting a grip on reality: Grasping movements directed to real objects and images rely on dissociable neural representations. *Cortex*, 98, 34-48.
- FREUD, E., PLAUT, D. C. & BEHRMANN, M. 2016. 'What' Is Happening in the Dorsal Visual Pathway. *Trends Cogn Sci*, 20, 773-84.
- FRISTON, K. 2009. Modalities, modes, and models in functional neuroimaging. *Science*, 326, 399-403.

- GOODALE, M. A. & MILNER, A. D. 1992. Separate visual pathways for perception and action. *Trends Neurosci*, 15, 20-5.
- GOODALE, M. A., MILNER, A. D., JAKOBSON, L. S. & CAREY, D. P. 1991. A neurological dissociation between perceiving objects and grasping them. *Nature*, 349, 154-156.
- GRILL-SPECTOR, K., KUSHNIR, T., HENDLER, T. & MALACH, R. 2000. The dynamics of object-selective activation correlate with recognition performance in humans. *Nature Neuroscience*, 3, 837-843.
- HAYNES, J. D. & REES, G. 2006. Decoding mental states from brain activity in humans. *Nature Reviews Neuroscience*, 7, 523-534.
- HEBART, M. N., GORGEN, K. & HAYNES, J. D. 2014. The Decoding Toolbox (TDT): a versatile software package for multivariate analyses of functional imaging data. *Front Neuroinform*, 8, 88.
- HESELNANN, G., DARCY, N., ROTHKIRCH, M. & STERZER, P. 2018. Investigating masked priming along the "vision-for-perception" and "vision-for-action" dimensions of unconscious processing. *J Exp Psychol Gen*, 147, 1641-1659.
- HESELNANN, G. & MALACH, R. 2011. The link between fMRI-BOLD activation and perceptual awareness is "stream-invariant" in the human visual system. *Cereb Cortex*, 21, 2829-37.
- JAMES, T. W., CULHAM, J., HUMPHREY, G. K., MILNER, A. D. & GOODALE, M. A. 2003. Ventral occipital lesions impair object recognition but not object-directed grasping: an fMRI study. *Brain*, 126, 2463-75.
- JEONG, S. K. & XU, Y. 2016. Behaviorally Relevant Abstract Object Identity Representation in the Human Parietal Cortex. *J Neurosci*, 36, 1607-19.
- JIMURA, K. & POLDRACK, R. A. 2012. Analyses of regional-average activation and multivoxel pattern information tell complementary stories. *Neuropsychologia*, 50, 544-52.
- KANWISHER, N. 2010. Functional specificity in the human brain: a window into the functional architecture of the mind. *Proc Natl Acad Sci U S A*, 107, 11163-70.
- KANWISHER, N., MCDERMOTT, J. & CHUN, M. M. 1997. The fusiform face area: A module in human extrastriate cortex specialized for face perception. *Journal of Neuroscience*, 17, 4302-4311.
- KASS, R. E. R., A.E. 1995. Bayes Factors. *Journal of the American Statistical Association*, 90, 773-795.
- KRIEGESKORTE, N., GOEBEL, R. & BANDETTINI, P. 2006. Information-based functional brain mapping. *Proceedings of the National Academy of Sciences of the United States of America*, 103, 3863-3868.
- LUDWIG, K., KATHMANN, N., STERZER, P. & HESSELNANN, G. 2015. Investigating category- and shape-selective neural processing in ventral and dorsal visual stream under interocular suppression. *Hum Brain Mapp*, 36, 137-49.
- LUDWIG, K., STERZER, P., KATHMANN, N. & HESSELNANN, G. 2016. Differential modulation of visual object processing in dorsal and ventral stream by stimulus visibility. *Cortex*, 83, 113-23.
- MACDONALD, S. N. & CULHAM, J. C. 2015. Do human brain areas involved in visuomotor actions show a preference for real tools over visually similar non-tools? *Neuropsychologia*, 77, 35-41.
- MARTINAUD, O. 2017. Visual agnosia and focal brain injury. *Rev Neurol (Paris)*, 173, 451-460.
- MELLONI, L., SCHWIEDRZIK, C. M., MULLER, N., RODRIGUEZ, E. & SINGER, W. 2011. Expectations change the signatures and timing of electrophysiological correlates of perceptual awareness. *J Neurosci*, 31, 1386-96.
- MILNER, A. D. 2017. How do the two visual streams interact with each other? *Exp Brain Res*, 235, 1297-1308.
- MOREY, R. D., ROUDER, J.N. 2015. Computation of Bayes Factors for Common Designs. 0.9.12-2 ed.
- MUR, M., BANDETTINI, P. A. & KRIEGESKORTE, N. 2009. Revealing representational content with pattern-information fMRI - an introductory guide. *SCAN*, 4, 101-109.
- PIOTROWSKI, L. N. & CAMPBELL, F. W. 1982. A demonstration of the visual importance and flexibility of spatial-frequency amplitude and phase. *Perception*, 11, 337-46.

- ROKEM, A., TAKEMURA, H., BOCK, A. S., SCHERF, K. S., BEHRMANN, M., WANDELL, B. A., FINE, I., BRIDGE, H. & PESTILLI, F. 2017. The visual white matter: The application of diffusion MRI and fiber tractography to vision science. *J Vis*, 17, 4.
- ROTH, Z. N. & ZOHARY, E. 2015. Fingerprints of Learned Object Recognition Seen in the fMRI Activation Patterns of Lateral Occipital Complex. *Cereb Cortex*, 25, 2427-39.
- SAN ROQUE, L., KENDRICK, K., NORCLIFFE, E., BROWN, P., DEFINA, R., DINGEMANSE, M., DIRKSMEYER, T., ENFIELD, N., FLOYD, S., HAMMOND, J., ROSSI, G., TUFVESSON, S., VAN PUTTEN, S. & MAJID, A. 2015. *Vision verbs dominate in conversation across cultures, but the ranking of non-visual verbs varies.*
- SCHENK, T. 2012. No dissociation between perception and action in patient DF when haptic feedback is withdrawn. *J Neurosci*, 32, 2013-7.
- SCHENK, T. & MCINTOSH, R. D. 2010. Do we have independent visual streams for perception and action? *Cognitive Neuroscience*, 1, 52-78.
- TAKEMURA, H., ROKEM, A., WINAWER, J., YEATMAN, J. D., WANDELL, B. A. & PESTILLI, F. 2016. A Major Human White Matter Pathway Between Dorsal and Ventral Visual Cortex. *Cereb Cortex*, 26, 2205-2214.
- TETTAMANTI, M., CONCA, F., FALINI, A. & PERANI, D. 2017. Unaware Processing of Tools in the Neural System for Object-Directed Action Representation. *J Neurosci*, 37, 10712-10724.
- TJAN, B. S., LESTOU, V. & KOURTZI, Z. 2006. Uncertainty and invariance in the human visual cortex. *J Neurophysiol*, 96, 1556-68.
- UNGERLEIDER, L. G. & MISHKIN, M. 1982. Two cortical visual systems. In: INGLE, D. J., GOODALE, M. A. & MANSFIELD, R. J. W. (eds.) *Analysis of visual behavior*. Cambridge, Massachusetts: MIT Press.
- VAN POLANEN, V. & DAVARE, M. 2015. Interactions between dorsal and ventral streams for controlling skilled grasp. *Neuropsychologia*, 79, 186-91.
- WINDEY, B., GEVERS, W. & CLEEREMANS, A. 2013. Subjective visibility depends on level of processing. *Cognition*, 129, 404-9.
- WU, W. 2014. Against Division: Consciousness, Information and the Visual Streams. *Mind & Language*, 29, 383-406.

Eidesstattliche Versicherung

„Ich, Natasha Darcy, versichere an Eides statt durch meine eigenhändige Unterschrift, dass ich die vorgelegte Dissertation mit dem Thema "Effects of stimulus degradation on neural object processing in the two visual pathways" selbstständig und ohne nicht offengelegte Hilfe Dritter verfasst und keine anderen als die angegebenen Quellen und Hilfsmittel genutzt habe.

Alle Stellen, die wörtlich oder dem Sinne nach auf Publikationen oder Vorträgen anderer Autoren beruhen, sind als solche in korrekter Zitierung kenntlich gemacht. Die Abschnitte zu Methodik (insbesondere praktische Arbeiten, Laborbestimmungen, statistische Aufarbeitung) und Resultaten (insbesondere Abbildungen, Graphiken und Tabellen werden von mir verantwortet.

Meine Anteile an etwaigen Publikationen zu dieser Dissertation entsprechen denen, die in der untenstehenden gemeinsamen Erklärung mit dem Betreuer angegeben sind. Für sämtliche im Rahmen der Dissertation entstandenen Publikationen wurden die Richtlinien des ICMJE (International Committee of Medical Journal Editors; www.icmje.org) zur Autorenschaft eingehalten. Ich erkläre ferner, dass mir die Satzung der Charité – Universitätsmedizin Berlin zur Sicherung Guter Wissenschaftlicher Praxis bekannt ist und ich mich zur Einhaltung dieser Satzung verpflichte.

Die Bedeutung dieser eidesstattlichen Versicherung und die strafrechtlichen Folgen einer unwahren eidesstattlichen Versicherung (§156,161 des Strafgesetzbuches) sind mir bekannt und bewusst.“

Datum

Unterschrift

Ausführliche Anteilserklärung an der erfolgten Publikation

Publikation 1: Natasha Darcy, Philipp Sterzer, Guido Hesselmann, Category-selective processing in the two visual pathways as a function of stimulus degradation by noise, NeuroImage, online erschienen am 25.12.2018, Printversion in der 188. Ausgabe im März 2019

Beitrag im Einzelnen:

- Konzeption: Definierung der Fragestellung aufgrund des aktuellen Forschungsstands, Planung des experimentellen Ablaufs, beides in enger Zusammenarbeit mit Guido Hesselmann
- Stimulusbilder: Bearbeitung von in der AG vorhandenen Stimulussets mit der SHINE Toolbox, Recherche der Noise-Methoden, Erstellen eines Skripts zum parametrischen Applikation von Bildrauschen mit Hilfe der Matlab Image Processing Toolbox, Auswertung der Bildstatistik
- Experiment: Erstellen der Skripte zur Darbietung der Stimuli und Erfassung der Antworten durch die Probanden auf Basis von vorhanden Skripten aus der Arbeitsgruppe; Planung und Durchführung der fMRT-Messungen im Berlin Center for Advanced Neuroimaging in Zusammenarbeit mit Peter Heinze
- Datenanalyse: Anpassen von bestehenden bzw. Erstellen neuer Analyseskripte zum Importieren von DICOMs, zur Präprozessierung, zur Einzel- und Gruppenanalyse der fMRT-Daten
- Statistik: selbstständige Analyse von Verhaltens- und fMRT-Daten in SPSS nach kurzer Einweisung durch Herrn Hesselmann; Erarbeiten der bayesianischen Statistik in R in Zusammenarbeit mit Herrn Hesselmann
- Manuskript: Verfassen des Manuskripts und des Supplements, Konzeption und Erstellung aller Figures, außerdem Revision und Beantwortung der Reviewerfragen; jeweils inhaltliche Kommentare und Korrekturlesungen von Guido Hesselmann und Philipp Sterzer

Unterschrift der Doktorandin

Journal Data Filtered By: **Selected JCR Year: 2017** Selected Editions: SCIE,SSCI
 Selected Categories: **“NEUROSCIENCES”** Selected Category Scheme: WoS
Gesamtanzahl: 261 Journale

Rank	Full Journal Title	Total Cites	Journal Impact Factor	Eigenfactor Score
1	NATURE REVIEWS NEUROSCIENCE	40,834	32.635	0.069940
2	NATURE NEUROSCIENCE	59,426	19.912	0.153710
3	ACTA NEUROPATHOLOGICA	18,783	15.872	0.041490
4	TRENDS IN COGNITIVE SCIENCES	25,391	15.557	0.040790
5	BEHAVIORAL AND BRAIN SCIENCES	8,900	15.071	0.010130
6	Annual Review of Neuroscience	13,320	14.675	0.016110
7	NEURON	89,410	14.318	0.216730
8	PROGRESS IN NEUROBIOLOGY	13,065	14.163	0.015550
9	BIOLOGICAL PSYCHIATRY	42,494	11.982	0.056910
10	MOLECULAR PSYCHIATRY	18,460	11.640	0.047200
11	JOURNAL OF PINEAL RESEARCH	9,079	11.613	0.008600
12	TRENDS IN NEUROSCIENCES	20,061	11.439	0.026860
13	BRAIN	52,061	10.840	0.075170
14	SLEEP MEDICINE REVIEWS	6,080	10.602	0.010720
15	ANNALS OF NEUROLOGY	37,251	10.244	0.053390
16	Translational Stroke Research	2,202	8.266	0.005260
17	NEUROSCIENCE AND BIOBEHAVIORAL REVIEWS	24,279	8.037	0.048460
18	NEUROSCIENTIST	4,738	7.461	0.008730
19	NEURAL NETWORKS	10,086	7.197	0.015290
20	FRONTIERS IN NEUROENDOCRINOLOGY	3,924	6.875	0.006040
21	NEUROPSYCHOPHARMACOLOGY	24,537	6.544	0.042870
22	CURRENT OPINION IN NEUROBIOLOGY	14,190	6.541	0.034670
23	Molecular Neurodegeneration	3,489	6.426	0.009850
24	CEREBRAL CORTEX	29,570	6.308	0.058970
25	BRAIN BEHAVIOR AND IMMUNITY	12,583	6.306	0.026850
26	BRAIN PATHOLOGY	4,952	6.187	0.007750
27	Brain Stimulation	4,263	6.120	0.014510
28	NEUROPATHOLOGY AND APPLIED NEUROBIOLOGY	3,654	6.059	0.006350
29	JOURNAL OF CEREBRAL BLOOD FLOW AND METABOLISM	19,450	6.045	0.028280
30	JOURNAL OF NEUROSCIENCE	176,157	5.970	0.265950
31	Molecular Autism	1,679	5.872	0.006320
31	Translational Neurodegeneration	589	5.872	0.002280
33	GLIA	13,417	5.846	0.020530
34	Neurotherapeutics	3,973	5.719	0.008980
35	PAIN	36,132	5.559	0.038000
36	NEUROIMAGE	92,719	5.426	0.152610
37	Acta Neuropathologica Communications	2,326	5.414	0.011550
38	Multiple Sclerosis Journal	10,675	5.280	0.021890

Publikation

Darcy, N., Sterzer, P., & Hesselmann, G. (2019). Category-selective processing in the two visual pathways as a function of stimulus degradation by noise. *Neuroimage*, *188*, 785-793.
doi:10.1016/j.neuroimage.2018.12.036

<http://www.doi.org/10.1016/j.neuroimage.2018.12.036>

Lebenslauf

Mein Lebenslauf wird aus datenschutzrechtlichen Gründen in der elektronischen Version meiner Arbeit nicht veröffentlicht.

Publikationsliste

Darcy, N., Sterzer, P., & Hesselmann, G. (2019). Category-selective processing in the two visual pathways as a function of stimulus degradation by noise. *Neuroimage*, *188*, 785-793. doi:10.1016/j.neuroimage.2018.12.036

Impact Factor: 5.426

Hesselmann, G., Darcy, N., Rothkirch, M., & Sterzer, P. (2018). Investigating masked priming along the "vision-for-perception" and "vision-for-action" dimensions of unconscious processing. *J Exp Psychol Gen*, *147*(11), 1641-1659. doi:10.1037/xge0000420

Impact Factor: 4.107

Hesselmann, G., Darcy, N., Ludwig, K., & Sterzer, P. (2016). Priming in a shape task but not in a category task under continuous flash suppression. *J Vis*, *16*(3), 17. doi:10.1167/16.3.17

Impact Factor: 2.266

Hesselmann, G., Darcy, N., Sterzer, P., & Knops, A. (2015). Exploring the boundary conditions of unconscious numerical priming effects with continuous flash suppression. *Conscious Cogn*, *31*, 60-72. doi:10.1016/j.concog.2014.10.009

Impact Factor: 2.272

Danksagung

Mein Dank gilt zuallererst meinen Doktorvätern, Guido Hesselmann und Philipp Sterzer, die mich für die Dauer der Einarbeitung in die Forschungsgruppe, der Durchführung meiner Experimente und der Niederschrift dieser wissenschaftlichen Arbeit fortwährend unterstützt haben. Ich lernte von Ihnen Vieles über authentische Wissenschaft und stets wohlgesinnte und starke Zusammenarbeit und hoffe, in meiner zukünftigen Arbeit einen ähnlich hohen Standard aufrecht zu erhalten. Danke Guido, für die wissenschaftlichen und wissenschaftsnahen Konversationen, die meine Stimmung erhellten und meine Interessen erweiterten.

Danken möchte ich zusätzlich der gesamten Arbeitsgruppe *Visuelle Wahrnehmung*, insbesondere Markus, Eyal, Peter, Juliane und Karin, für den kollegialen und offenen wissenschaftlichen Austausch, der meine Projekte bereicherte.

Ein besonderer Dank gilt meinen Eltern, die mich bedingungslos in all meinen Unternehmungen unterstützen. Auch dankbar bin ich für die Freundschaften und den moralisch stärkenden Austausch mit meinen Kommilitoninnen und Kommilitonen.